Proceedings of the 42nd IEEE
Conference on Decision and Control
Maui, Hawaii USA, December 2003

Control, Observation and Energy Regulation of Wake Flow Instabilities

Gilead Tadmor
Electrical & Comp. Eng.
Northeastern University
Boston, MA 02115, USA.
tadmor@ece.neu.edu

Bernd R. Noack and
Andreas Dillmann
Hermann-Föttinger-Institute
of Fluid Mechanics
Techn. Univ. Berlin
Straße des 17 Juni 135
D-10623 Berlin, Germany

Johannes Gerhard,
Mark Pastoor and
Rudibert King
Measurement & Control Gr.
Institute for Process
and Plant Technology
Techn. Univ. Berlin
Hardenbergstraße 36a
D-10623 Berlin, Germany

Marek Morzyński
Inst. Combust. Engines &
Basics of Machine Design
Poznań Univ. Techn.
ul. Piotrowo 3,
PL 60-965 Poznań, Poland

Abstract— **A three-dimensional Galerkin model is used in feedback design to regulate the perturbation kinetic energy in the flow around a cylinder. The objective may vary from stabilization in order to reduce drag to mixing enhancement. The Landau model [1] includes an oscillatory state pair and a shift mode, exchanging energy with the mean flow. Given the model's simplicity, it is essential to maintain closed-loop dynamics close to the system's natural dynamic range which is represented by an invariant manifold and a natural frequency, adding a design constraint addressed in this note.**

I. The Problem

The complexity of computational fluid dynamics (CFD) models is a major hindrance to implementable feedback control [2]. This note presents a benchmark design based on a very low order Galerkin model and highlights control design aspects peculiar to the use of such models. The regulation of laminar vortex shedding behind a cylinder has been adopted as our benchmark control problem from the fluid flow community [3]- [6]. The system is considered at the reference Reynolds number of 100 which is far above the laminar shedding regime's critical value of 47 [7] but far below the transitional range in which three-dimensional instabilities characterize the flow [8]. This paper is focused on the control and system theoretic aspects. Model development issues are discussed in [9], [10] and we shall therefore be content here with a brief review.

Reduced order Galerkin models (GM) are widely used in fluid dynamics [11]. Here, the GM utilizes an orthonormal[1] Galerkin approximation of the attractor

$$\mathbf{u}(\mathbf{x},t) = \mathbf{u}_s(\mathbf{x}) + \sum_{i=1}^{3} a_i(t)\,\mathbf{u}_i(\mathbf{x}), \tag{1}$$

where $\mathbf{u}_s(\mathbf{x})$ is the unstable steady Navier-Stokes solution and the Karhunen-Loève modes $\mathbf{u}_i(\mathbf{x})$, $i = 1, 2$, capture some 96% of the perturbation energy of the von Kármán oscillatory instability. Yet, a model based on these two modes alone cannot capture any of the system dynamics. That is the purpose of the *shift mode* $\mathbf{u}_3(\mathbf{x}) \propto \mathbf{u}_s(\mathbf{x}) - \mathbf{u}_0(\mathbf{x})$ which is an orthonormalized mean-field correction between the natural mean flow $\mathbf{u}_0(\mathbf{x})$ and the steady solution. This shift mode resolves the energy exchange between the base flow and the oscillatory perturbation. Figure 1 depicts these four modes in terms of stream-lines. Actuation is effected with a local volume force, $\mathbf{f}(\mathbf{x})$, in the near-wake, thus mimicking, for instance, a Lorentz force in a magneto-hydrodynamical flow. Both a single and a two degrees of freedom actuation, are considered. In the former case, the orientation of the force is fixed: $\mathbf{f}(\mathbf{x}) = \alpha_1\mathbf{u}_1(\mathbf{x}) + \alpha_2\mathbf{u}_2(\mathbf{x})$, with fixed α_i. This ansatz ignores the residual field which is left out of the GM model. In the latter case, two identically structured actuators will stimulate mutually orthogonal fields, $\mathbf{f}_i(\mathbf{x})$, $i = 1, 2$. A single or multiple point velocity field sensor (such as hot-wire anemometers), captured by the variable s, are postulated, located sufficiently far downstream and displaced from the axis of symmetry near the maximum of fluctuation energy. As will be seen below, velocity field transients are dominated by a single harmonic, which is therefore easily identifiable. Under slow variations in $a_3(t)$ (relative to the dominant period), residual effects of both the constant $\mathbf{u}_s$ and the slowly varying $a_3\mathbf{u}_3$, can be removed by band-pass filtering. It is thus assumed that, excluding noise, the sensor reading s is a linear combination of a_1 and a_2. Figure 2 depicts the system with a single actuator and a single sensor.

Under this description, the Galerkin system is given by

$$\dot{a} = A(a)a + B\epsilon, \quad s = Ca \tag{2}$$

where $a := [a_1, a_2, a_3]^T$, ϵ is the actuation command, and

$$A(a) := \begin{bmatrix} \mu & -\omega & -\beta a_1 \\ \omega & \mu & -\beta a_2 \\ \delta a_1 & \delta a_2 & -\rho \end{bmatrix} \tag{3}$$

The coupling terms βa_i and δa_i and the growth parameter $\mu > 0$ are typically small relative to the natural oscillation frequency ω and dissipation parameter $\rho > 0$. A single actuator is represented by a scalar ϵ and $B = b[\cos(\theta), \sin(\theta), 0]^T$. Associated with a double actuator, $\epsilon := [\epsilon_1, \epsilon_2]^T$, and $B = b\begin{bmatrix} \cos(\theta) & -\sin(\theta) \\ \sin(\theta) & \cos(\theta) \\ 0 & 0 \end{bmatrix}$ reflects the assumed orthogonal symmetry of the two volume force fields. The sensor coefficient for a single sensor is $C = [c_1, c_2, 0]$. With multiple sensors, the matrix C will comprise several rows of a similar form.

The control task set forth is the design of feedback regulation of the perturbation kinetic energy, represented by $K(t) = 0.5\|a(t)\|^2$, about a set reference, $K_\star$. Stabilization of the reference $K_\star = 0$ is most commonly discussed, motivated by such objectives as reducing drag or mechanical vibrations. Enhancement of K beyond its open loop value may be motivated by a mixing objective.

An energy regulation objective, respects the basic characteristics of the system's unactuated, oscillatory dynamics — as opposed to other setpoint or orbit tracking tasks. Indeed, an intrinsic limitation

[1] Signal norms (with the subscript "2"), inner products and orthogonality is understood in the appropriate (spatial or temporal) L_2 sense. Euclidean norms (with no subscript) and inner products are used for Euclidean vectors. To simplify notations, the base flows $\mathbf{u}_0$ and $\mathbf{u}_s$ are *not* normalized in (1) and elsewhere

0-7803-7924-1/03/$17.00 ©2003 IEEE

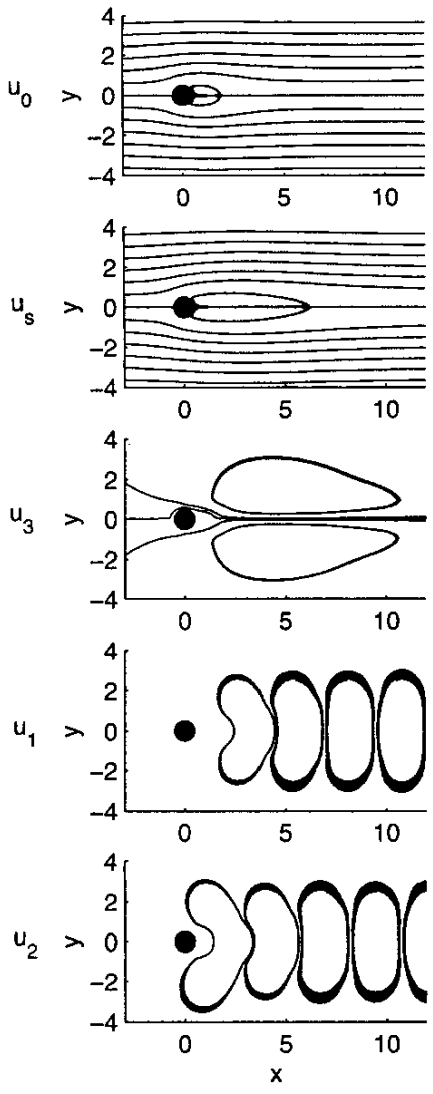

Fig. 1. *Galerkin approximation. The mean-flow* $\mathbf{u}_0$*, the steady solution* $\mathbf{u}_s$*, the shift-mode* $\mathbf{u}_3$*, and the Karhunen-Loève modes* $\mathbf{u}_1$, $\mathbf{u}_2$ *are visualized (top to bottom) with stream-lines.*

of almost any reduced order model of a truly distributed and / or nonlinear system is its restriction to an often narrow envelope of state values and dynamic range. This certainly applies as a generic aspect to any attempt at feedback control design based on reduced order models of fluid flow systems. As has been repeatedly demonstrated in other contexts, as well as in this very example, an aggressive and theoretically effective control that ignores such constraints can result with mode shifts that will render the Galerkin system and the reduced order model irrelevant, and lose its effectiveness in the real system. A second, equally essential design objective, that is likely to characterize any control design in low order flow models, is therefore to maintain closed loop behavior near its natural range, and an analysis of the meaning of this objective is an important part of the overall design task.

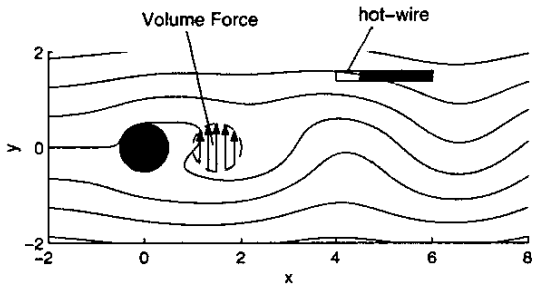

Fig. 2. Stream-lines of the natural flow around a circular cylinder. The location of the volume force is illustrated by a circle and a single hot-wire anemometer is on one side of the von Kármán vortex street.

II. State Feedback & Constraints

To better understand the dynamics of (2), relative to energy regulation, it is useful to transition to polar coordinates $[a_1, a_2]^T = [\cos(\phi), \sin(\phi)]^T r$, whereby $K = 0.5(r^2 + x_3^2)$. In these terms

$$\begin{bmatrix} \dot{r} \\ \dot{a}_3 \end{bmatrix} = \begin{bmatrix} \mu & -\beta r \\ \delta r & -\rho \end{bmatrix} \begin{bmatrix} r \\ a_3 \end{bmatrix} + b \begin{bmatrix} g_r(\phi) \\ 0 \end{bmatrix} \epsilon \qquad (4)$$

$$\dot{\phi} = \omega + \frac{b}{r} g_p(\phi) \epsilon \qquad (5)$$

In the single actuator system, the terms g_r and g_p are the scalars $g_r(\phi) = \cos(\theta - \phi)$ and $g_p(\phi) = \sin(\theta - \phi)$. In the dual actuator system, g_r and g_p are orthogonal vector valued, $g_r(\phi) = [\cos(\theta - \phi), -\sin(\theta - \phi)]$ and $g_p(\phi) = [\sin(\theta - \phi), \cos(\theta - \phi)]$ (and the zero in the second row of the forcing term, in (4), is interpreted as the zero row, [0, 0]).

Characteristics of unactuated dynamics ($\epsilon \equiv 0$) are now easy to see [1]: Oscillations between a_1 and a_2 are at the fixed frequency of ω. Concerning energy dynamics, the origin, $K = 0$, is an unstable saddle point. A stable rest point for (4) exists at $r^2 = \frac{\rho}{\delta} a_3 = \frac{\rho\mu}{\delta\beta}$, corresponding to a stable (phase-shift invariant) limit cycle, in (2). The magnitude gap between ρ and μ, and weak coupling ($\Leftrightarrow \beta r$ and δr small relative to ρ) translate to slow dynamics in r and much faster convergence of a_3. This allows an approximation of the invariant manifold, connecting the unstable rest point and the limit cycle, based on time constant separation, with rapid convergence of a_3 to $\frac{\delta}{\rho} r^2$.

Design guidelines, based on the desire to remain near the system's natural dynamic range, are derived from these characteristics. Roughly stated, they include:

1) A restriction to slow changes in r, and
2) Small perturbation of the rotation frequency, $\dot{\phi} \approx \omega$.

Implications are analyzed separately in the single and dual actuator cases.

The dual actuator case. A starting point is the observation that $\forall \phi$, $g_r(\phi) \perp g_p(\phi)$ in $\mathbb{R}^2$. Thus, the objective to effect energy dynamics and avoid phase actuation, is easily achieved, orienting $\epsilon(t) = g_r(\phi)^T \eta(t)$, with a scalar $\eta(t)$. Consequently, the actuated system becomes

$$\begin{bmatrix} \dot{r} \\ \dot{a}_3 \end{bmatrix} = \begin{bmatrix} \mu & -\beta r \\ \delta r & -\rho \end{bmatrix} \begin{bmatrix} r \\ a_3 \end{bmatrix} + \begin{bmatrix} b \\ 0 \end{bmatrix} \eta \qquad (6)$$

$$\dot{\phi} = \omega \qquad (7)$$

Noting that the relation $a_3 = \frac{\delta}{\rho} r^2$ must be maintained at any steady state, a constant reference K_* readily translates to references

r_* and $a_{3*} = \frac{\delta}{\rho} r_*^2$, satisfying $K_* = 0.5(r_*^2 + a_{3*}^2)$, and to a steady state control

$$\epsilon_* = g_r(\phi)^T \eta_*, \quad \eta_* = (\beta a_{3*} - \mu) r_* / b \tag{8}$$

This last equation reveals, in particular, one connection between actuation amplitude limits and performance limits. Performance limits are further discussed later on.

Denoting deviations from steady state by $\triangle$, transient dynamics can be represented as

$$\begin{bmatrix} \triangle \dot{r} \\ \triangle \dot{a}_3 \end{bmatrix} = \begin{bmatrix} \mu - \beta a_{3*} & -\beta r \\ \delta(r + r_*) & -\rho \end{bmatrix} \begin{bmatrix} \triangle r \\ \triangle a_3 \end{bmatrix} + \begin{bmatrix} b \\ 0 \end{bmatrix} \triangle \eta \tag{9}$$

An incremental control, $\triangle \epsilon = g_r(\phi)^T \triangle \eta$, must be added to ϵ_*, to stabilize the reference point. One *incrementally dissipative control design* to attenuate the tracking error, is

$$\triangle \eta = \frac{1}{b}((\beta a_{3*} - \mu - \kappa)\triangle r + \beta r \triangle a_3) \tag{10}$$

where $\kappa > 0$ is a design parameter. The feedback (10) shapes closed loop error dynamics as a cascade

$$\begin{bmatrix} \triangle \dot{r} \\ \triangle \dot{a}_3 \end{bmatrix} = \begin{bmatrix} -\kappa & 0 \\ \delta(r + r_*) & -\rho \end{bmatrix} \begin{bmatrix} \triangle r \\ \triangle a_3 \end{bmatrix} \tag{11}$$

Indeed, (10) was selected to provide complete control of the rate of convergence in r in terms of the design parameter κ. Thus, (10) facilitates adherence to the requirement of slow convergence in r. To further impose an absolute bound over $\triangle \dot{r}$, one saturates $\kappa \triangle r$, in (10).

The single actuator case: A first approximation. The obvious disadvantage, here, is that now $g_r(\phi) = \cos(\theta - \phi)$ and $g_p(\phi) = \sin(\theta - \phi)$ take scalar values, and cannot be instantaneously orthogonal. Nonetheless, under nearly periodic dynamics (either due to low gain actuation, or deliberate design), these two coefficients are nearly L_2-orthogonal over a period. Actuation aimed to be restricted to energy dynamics, and to minimize effects on the phase, must therefore be in phase with $g_r(\phi)$, and L_2 - orthogonal to $g_p(\phi)$.

A natural option that may come to mind is $\epsilon = g_r(\phi)\eta$, with a slowly varying η. Its advantage is in a smooth, nearly sinusoidal actuation force. Its main drawback is that it does not maximize available gain over a period. A second example, addressing the gain issue, is the nearly square wave, $\epsilon = \frac{\pi}{2}\text{sign}(\cos(\theta - \phi))\eta$. The respective forcing terms are then of the form $b g_r(\phi)\epsilon = b(1 + h_r(\phi))\eta$, and $b g_p(\phi)\epsilon = b\, h_p(\phi)\eta$, where $h_r(\phi)$ and $h_p(\phi)$ are zero–mean harmonic terms. Thus, here, $b g_r \epsilon$ averages over a period to $b\eta$, and $b g_p \epsilon$, to zero. Equations (6) and (7) then provide a rough approximate dynamic model for period averages (upon which we improve below). The control policy (8)-(10) can then be used for the selection of η.

Here it should be stressed that now the objective of imposing slow convergence in r is also necessary to maintain the rationale for the suggested policy, which hinges on the fact that the underlying dynamics is nearly periodic, hence that η is slowly varying. Also noted are the following disadvantages of the single actuator. First, to achieve the same (averaged effect), the peak magnitude of the actuation signal must be higher: in the dual actuator system $\|g_r \epsilon\| \equiv b|\eta|$, whereas in the single actuator system, $g_r \epsilon = b\frac{\pi}{2}\text{sign}(\cos(\theta - \phi))\eta$ leads to a ratio of $2b : \pi$ – some 32% lower – between the peak amplitude of ϵ and average value of $g_r \epsilon$. Actuation amplitude limitations therefore result with a more stringent effective gain limitation, in this case. A second disadvantage is due to the fact that, even though the desired energy level K_*, and the constraint $\frac{d}{dt}\phi \approx \omega$, are maintained *on average*, harmonics in the actuation terms necessarily imposes harmonic deviations from the set value in both. Harmonic distortions in the rotation frequency will grow in reverse proportion to a decline in r, due to the form of the forcing term in (5), although the significance of such harmonics distortions may then diminish, due to the same decline.

Remark. Our benchmark exhibits here two generic attributes of fluid flow control: dominant oscillatory structures and similar structures under actuation. Our selected approach, which too might prove to be of generic value (see also [12], [13]), is a design aimed to control selected phasors (= Fourier coefficients) rather then instantaneous response, utilizing functions space (here, moving window L_2) geometry, rather than instantaneous Euclidean geometry, to effect designated variables, and avoid others. This approach hinges on maintaining near-periodicity.

The single actuator: added details. *For simplicity, detailed computations are presented for the case $\rho = \beta = \delta = \omega = 1$.*

There are two options in planning and scaling the actuation input for a period (or half a period) ahead: One option is to scale the amplitude of the actuation input; the other is to scale the time interval over which a non zero actuation is applied. Denoting by t_k the time where $\phi(t_k) - \theta = (k - 0.5)\pi$, in both cases we shall discuss a discrete time decision process, where control commands are issued at the time t_k for the interval $[t_k, t_{k+1}]$ (i.e., for the next interval over which $\cos(\phi - \theta)$ maintains a constant sign). At nearly constant frequency, the step size remains $\triangle t := t_{k+1} - t_k \approx \pi$. Under this assumption we shall now explore the two scaling options.

1. A scaled constant actuation over a half period. The control input during the interval $[t_k, t_{k+1}]$ will be a constant, ϵ_k. An approximation of $r(t_{k+1})$ in terms of $r(t_k)$ and ϵ_k can be obtained, substituting the term $\mu - \beta a_3$ in (4) by the constant $\mu_k = \mu - \beta a_3(t_k)$, and predicting $t_{k+1} = t_k + \pi$. A straightforward solution of the resulting version of (4), reveals

$$r(t_{k+1}) \approx e^{\mu_k \pi} r(t_k) + \frac{(-1)^k}{\mu_k^2 + 1}(e^{\mu_k \pi} + 1)\epsilon_k \tag{12}$$

To obtain $r(t_{k+1}) = \sigma r(t_k)$, $\sigma \in (0, 1)$, one therefore sets

$$\epsilon_k = (-1)^{k+1} \frac{\mu_k^2 + 1}{e^{\mu_k \pi} + 1}(e^{\mu_k \pi} - \sigma) r(t_k) \tag{13}$$

The effect of this selection on the oscillation frequency of the von Kármán modes is captured by

$$\dot{\phi} = 1 - \frac{1}{r}\sin(\phi - \theta)\epsilon_k \tag{14}$$

Since the integration is over an interval where $\phi - \theta$ traverses $[(k - 0.5)\pi, (k + 0.5)\pi]$, if one can ignore variations in $1/r$, the average impact on $\frac{d}{dt}\phi$ will be small. However, these approximations will deteriorate for small values of r.

2. A scaled period of actuation. Here we adopt a *bang-bang control* approach, whereby admissible values of ϵ are 0 and $\pm\epsilon_0$, and

switching is determined by a control parameter, ζ_k:

$$\epsilon_k(t) = \begin{cases} 0 & t \in [t_k, t_k + 0.5\pi - \zeta_k] \\ (-1)^k sign(r^* - r)\epsilon_0 & t \in [t_k + 0.5\pi - \zeta_k,\ t_k + 0.5\pi + \zeta_k] \\ 0 & t \in [t_k + 0.5\pi + \zeta_k,\ t_{k+1}] \end{cases} \quad (15)$$

Note that the advantage of this switching policy is that non zero actuation is concentrated near the points $\phi - \theta = k\pi$, where the impact of the actuation signal on ϕ is minimal, while the impact on $\dot{r}$ is maximal.

Direct application of the variations of constants formula in the simplified (4), as was done above, leads to the approximation

$$\begin{aligned} r(t_{k+1}) \approx\ & e^{m_k \pi} r(t_k) \\ & + e^{m_k(0.5\pi - \zeta_k)}(\sin(\zeta_k) + \mu_k \cos(\zeta_k)) \\ & + e^{m_k(0.5\pi + \zeta_k)}(\sin(\zeta_k) - \mu_k \cos(\zeta_k)) \end{aligned} \quad (16)$$

The parameter ζ_k is selected so that $r(t_{k+1}) = \sigma r(t_k)$, for a selected decay constant $\sigma \in (0, 1)$, as above. While a closed form expression is not available for the dependence $\zeta_k(\mu_k) = \zeta_k(\mu - a_3(t_k))$ (once σ is fixed), it can be easily computed and stored in a lookup table.

Limits due to actuation amplitude bounds. We have already made note of the obvious way in which amplitude constraints on feasible values of η_* translate to constraints on the feasibility of reference levels of K_*. Additional constraints are due to transient input levels. Transients have to be analyzed since disturbance induced deviations from unstable reference points – brief as they might be – ought to be expected. We shall be content with comments on the case $K_* = 0$ (stabilization), as other cases are analyzed similarly. Here, $a_{3*} = r_* = \eta_* = 0$ and thus $r = \triangle r$, $a_3 = \triangle a_3$ and $\eta = \triangle \eta$. Appealing again to the approximation $a_3 \approx \frac{\delta}{\rho} r^2$ (based on time constant separation), (10) becomes

$$\eta = \frac{1}{b}\left(\frac{\beta\delta}{\rho} r^2 - \mu - \kappa\right) r \quad (17)$$

The maximum amplitude of η can thus be evaluated over the range of $r \in \left[0, \sqrt{\rho\mu/\beta\delta}\right]$, covering the transient from the attractor to the steady flow. Similarly simple consideration may be used to analyzed the feasibility of maintaining the system at any other reference point for K, under actuation amplitude constraints.

III. Observer Design

Observer-based control combines a state feedback scheme, as described above, and a state estimate, which is the topic of this section.

A Single Sensor Observer Design. The sensor signal is $s(t) = Ca = c_1 a_1(t) + c_2 a_2(t)$. A simple rotation in the subspace $sp\{a_1, a_2\}$ leaves the structure of (2) intact, but brings the coefficient C to the form $C = [\tilde{c}_1, 0, 0]$. We therefore continue without any loss of generality, discussing only the case where $c_1 > 0$ and $c_2 = 0$. This amounts to direct measurement of a_1.

Observer design begins with (2) and a yet undetermined correction vector d

$$\frac{d}{dt}\widehat{a} = \begin{bmatrix} \mu & -\omega & -\beta a_1 \\ \omega & \mu & -\beta\widehat{a}_2 \\ \delta a_1 & \delta\widehat{a}_2 & -\rho \end{bmatrix} \begin{bmatrix} a_1 \\ \widehat{a}_2 \\ \widehat{a}_3 \end{bmatrix} + B\epsilon - d \quad (18)$$

A dynamic model for the propagation of the estimation error, $\triangle a := a - \widehat{a}$, linearized near $\triangle a = 0$ is

$$\frac{d}{dt}\triangle a = \begin{bmatrix} 0 & -\omega & -\beta a_1 \\ 0 & \mu - \beta\widehat{a}_3 & -\beta\widehat{a}_2 \\ 0 & 2\delta\widehat{a}_2 & -\rho \end{bmatrix} \triangle a + d \quad (19)$$

Available information is the measured error $\triangle a_1$, meaning that the first column in the matrix coefficient, in (19), can be freely assigned. Explicitly, our selection is

$$h = \begin{bmatrix} -2\kappa - \mu \\ \kappa^2\omega \\ \kappa^2\delta a_1 \end{bmatrix} \triangle a_1 \quad (20)$$

where $\kappa > 0$ is the design parameter. Under this selection, (19) becomes

$$\frac{d}{dt}\triangle a = \begin{bmatrix} -2\kappa - \mu & -\omega & -\beta a_1 \\ \kappa^2\omega & \mu - \beta\widehat{a}_3 & -\beta\widehat{a}_2 \\ 2\kappa^2\delta a_1 & 2\delta\widehat{a}_2 & -\rho \end{bmatrix} \triangle a \quad (21)$$

To clarify the effect of this form, consider the dynamics of the weighted error $\xi = [\triangle a_1, \frac{1}{\kappa}\triangle a_2, \frac{\sqrt{\beta}}{\sqrt{2\delta}\kappa}\triangle a_3]^T$. (Equivalently, consider (21) with the stored energy defined as $\triangle E := 0.5(\triangle a_1^2 + \frac{1}{\kappa^2}\triangle a_2^2 + \frac{\beta}{2\delta\kappa^2}\triangle a_3^2)$.)

$$\frac{d}{dt}\xi = \begin{bmatrix} -2\kappa - \mu & -\kappa\omega & -\sqrt{2\beta\delta}\kappa\widehat{a}_1 \\ \kappa\omega & \mu - \widehat{a}_3 & -\sqrt{2\beta\delta}\widehat{a}_2 \\ \sqrt{2\beta\delta}\kappa\widehat{a}_1 & \sqrt{2\beta\delta}\widehat{a}_2 & -\rho \end{bmatrix} \xi \quad (22)$$

where the off-diagonal terms in the matrix coefficient define a skew symmetric matrix, meaning that the dynamics they create is conservative. Since the diagonal contains both negative and positive terms, stability is not immediate. The following is a heuristic argument, beginning with the top left 2×2 block. By selecting κ sufficiently large, terms in μ and $\mu - \widehat{a}_3$ can be considered as small perturbations, and stability properties can be deduced from stability properties of the time invariant matrix where these terms are eliminated: $\kappa \begin{bmatrix} -2 & -1 \\ 1 & 0 \end{bmatrix}$. This block is uniformly exponentially stable with two eigenvalues placed at $-\kappa$. Moreover, it is dissipative relative to the Euclidean norm of the state. As the autonomous dynamics of ξ_3 is dissipative and energy exchange between $[\xi_1, \xi_2]^T$ and ξ_3 is conservative, the combined system is stable.

The tradeoff in selecting a large observer gain should not be overlooked, however: in addition to basic considerations of avoiding amplification of sensor noise, it is noted that the energy construct for estimation errors discounts the unknown errors in $\widehat{a}_2$ and $\widehat{a}_3$, as they are divided by κ.

A second approach that we mention only very briefly, is similar to the one elaborated in [13]. Maintaining the "near periodicity" assumption, the dynamics of a_1 is nearly sinusoidal with a slowly varying amplitude. A simple extended Kalman filter readily translates measurements of a_1 into estimates of both its amplitude r and phase ϕ. All that is left, now, is to estimate the slowly varying a_3 based on the estimated r and ϕ. A crude estimate would be $\widehat{a}_3 = \frac{\delta}{\rho}\widehat{r}^2$. An alternative is to proceed with the "multiple sensor observer" below, to estimate a_3.

Multiple Sensors Observers. Here we assume the presence of two

or more sensors, hence C has the form

$$C = \begin{bmatrix} c_{11} & c_{12} & 0 \\ c_{21} & c_{22} & 0 \\ \vdots & & \\ c_{k1} & c_{k2} & 0 \end{bmatrix} \tag{23}$$

If sensors are placed so that the column rank of C is 2, the vector $[a_1, a_2]^T$ can be recovered (or least-mean-squares estimated) from s. This means both that the very need for a dynamic observer is greatly reduced and that observer design can be simpler. Indeed, only a_3 now needs to be estimated and, in fact, an observer is altogether redundant if only *bang-bang* feedback control is implemented.

Having a measurement of both a_1 and a_2 implies, in particular, a measurement of r, and the observer will be based on the slow dynamics of (4).

$$\frac{d}{dt}\begin{bmatrix} \widehat{r} \\ \widehat{a}_3 \end{bmatrix} = \begin{bmatrix} \mu & -\beta r \\ \delta r & -\rho \end{bmatrix}\begin{bmatrix} r \\ \widehat{a}_3 \end{bmatrix} - d \tag{24}$$

Since we use the measured value of r, the estimator has a linear parameter varying structure and a correspondingly simple error dynamics

$$\frac{d}{dt}\begin{bmatrix} \triangle r \\ \triangle a_3 \end{bmatrix} = \begin{bmatrix} 0 & -\beta r \\ 0 & -\rho \end{bmatrix}\begin{bmatrix} \triangle r \\ \triangle a_3 \end{bmatrix} + d \tag{25}$$

The correction term, modifying the first column in the "A" matrix, can be selected as

$$d = \begin{bmatrix} -\nu \\ \lambda^2 \beta r \end{bmatrix} \triangle r \tag{26}$$

leading to the closed loop dynamics

$$\frac{d}{dt}\begin{bmatrix} \triangle r \\ \triangle a_3 \end{bmatrix} = \begin{bmatrix} -\nu & -\beta r \\ \lambda^2 \beta \delta r & -\rho \end{bmatrix}\begin{bmatrix} \triangle r \\ \triangle a_3 \end{bmatrix} \tag{27}$$

It is easily observed that this system is strictly dissipative relative to the storage function $\triangle E = 0.5(\lambda^2 \triangle r^2 + \triangle a_3^2)$, hence uniformly exponentially stable. Concerning design parameter assignments, if the reference $r^* \neq 0$ then values of ν and λ can be balanced to place the two eigenvalues of (25) at the same, desired location (i.e., determining a single convergence time constant). If $r^* = 0$, the ability to manipulate convergence rate diminishes as $r \mapsto 0$. A selection of design parameters can thus be guided by pole placement at a point away from the target, such as at an anticipated initial point of the control task (say, at the stable limit cycle).

Open and closed loop trajectories are depicted in Figure 3.

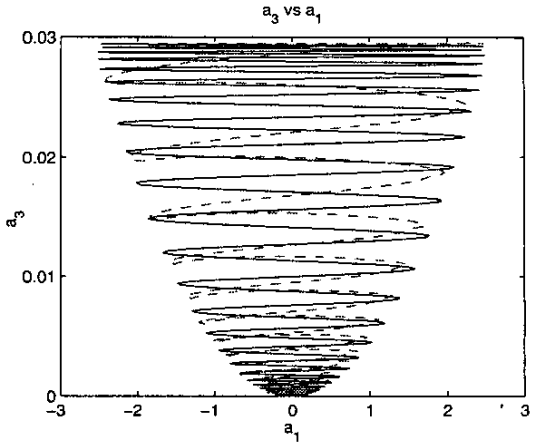

Fig. 3. Natural and controlled transients in state space. The natural and controlled trajectories are shown as solid, blue line (–) and dashed, red line actuated (- -). Evidently, both transients stay on the same paraboloid: the natural transient leaves the fixed point whereupon the control transient approaches the fixed point.

IV. Concluding Remarks

The benchmark discussed in this note features several generic aspects of what is hopefully evolving into a viable methodology of low-order, model-based feedback design in fluid flow systems. The reduced-order model is focused on large coherent structures, dominated by rotating modes as well as an added physics-based (shift) mode. The combination of standard proper orthogonal decomposition (POD) methods [11] and physical insight enables to capture a large proportion of the perturbation energy over a dynamic range that includes the transients of interest (as opposed to the common focus on a single operating point). Nonetheless, the model is still restricted to a relatively narrow envelope, which control and observer design must respect – and may wisely utilize. In the example at hand, that envelope is characterized by a fixed rotation frequency and slow variations in the kinetic energy level of the perturbation signal. Even in the case of a single actuator, this periodicity enables to achieve function space orientation, directed at phenomena we wish to control (energy level), and avoiding those we wish to leave unaffected (phase dynamics). The fact that Galerkin models are based on quadratic Hamiltonian dynamics is reflected by the relative ease at which incrementally dissipative design can address both control and observation. Moreover, as noted (without elaboration), an even simpler dynamic observer is feasible, based on an extended Kalman filter tracking of a nearly sinusoidal sensed signal. This kind of harmonic tracking observers seem to be natural in diverse examples, and have been previously applied in vortex systems, as well.

In closing, it is noted that spatial mode shift, that is, a drift from $\mathbf{u}_i(\mathbf{x})$ to $\mathbf{u}_i(\mathbf{x} - \mathbf{x}_0)$, with an unknown local $\mathbf{x}_0$, is an observed phenomenon in the wake flow, especially, under aggressive actuation. An additional, potential advantage and an interesting topic for further research is the possibility to utilize multiple sensor measurements to estimates $\mathbf{x}_0$ and make appropriate corrections in the actuation.

Acknowledgment

This research was supported by the US National Science Foundation (NSF) and by the Deutsche Forschungsgemeinschaft (DFG) via the Collaborative Research Center (Sfb557) "Control of complex turbulent shear flows".

V. References

[1] H.K. Khalil (2002) *Nonlinear Systems.* Prentice Hall, 3rd edition.

[2] T.R. Bewley & S. Liu (1998) Optimal and robust control and estimation of linear paths to transition, *J. Fluid Mech.* **365**, 305–349

[3] M.F. Unal & D. Rockwell (1987) On the vortex formation from a cylinder; Part 2. control by a splitter-plate interference, *J. Fluid Mech.* **190**, 513–529

[4] P.J. Strykowski & K.R. Sreenivasan (1990) On the formation and suppression of vortex 'shedding' at low Reynolds numbers, *J. Fluid Mech.* **218**, 71–107

[5] E. DETEMPLE-LAAKE & H. ECKELMANN (1989) Phenomenology of Kármán vortex streets in oscillatory flow, *Exps. Fluids* **7**, 217–227

[6] K. ROUSSOPOULOS (1993) Feedback control of vortex shedding at low Reynolds numbers, *J. Fluid Mech.* **248**, 267–296

[7] M. MORZYŃSKI, K. AFANASIEV & F. THIELE (1999) Solution of the eigenvalue problems resulting from global non-parallel flow stability analysis, *Comput. Meth. Appl. Mech. Enrgrg.* **169**, 161–176

[8] M.M. ZDRAVKOVICH (1997) *Flow Around Circular Cylinders, Volume 1: Fundamentals*, Oxford University Press, Oxford.

[9] B.R. NOACK, K. AFANASIEV, M. MORZYŃSKI, G. TADMOR & F. THIELE (2003) A hierarchy of low-dimensional models for the transient and post-transient cylinder wake. To appear in *J. Fluid Mech.*

[10] J. GERHARD, M. PASTOOR, R. KING, B. R. NOACK, A. DILLMANN, M. MORZYŃSKI & G. TADMOR (2003) Model-based control of vortex shedding using low-dimensional Galerkin models, *AIAA Paper* **2003-4262**.

[11] P. HOLMES, J.L. LUMLEY & G. BERKOOZ (1998) *Turbulence, Coherent Structures, Dynamical Systems and Symmetry*, Cambridge University Press, Cambridge.

[12] G. TADMOR & A. BANASZUK (2002) Observation feedback control of vortex motion in a recirculation region, *IEEE Trans. Control Sys. Tech.* **10**, 749 – 755

[13] G. TADMOR (2002) Feedback control of a rotating vortex pair, *The 2002 American Physical Society Division of Fluid Dynamics Annual Meeting*, **Bull. Am. Phys. Soc. 47**.

[14] R. LOZANO, B. BROGLIATO, O. EGELAND & B. MASCHKE (2000) *Dissipative Systems Analysis and Control: Theory and Applications*, Springer Verlag.